Flexibility of Myosin Attachment to Surfaces Influences F-Actin Motion

Donald A. Winkelmann,* Laurent Bourdieu,‡ Albrecht Ott,§ Fumi Kinose,* and Albert Libchaber‡§

*Department of Pathology, Robert Wood Johnson Medical School, Piscataway, New Jersey 08854; ‡Rockefeller University, New York, New York 40021; and §NEC Research Institute, Princeton, New Jersey 08540 USA

ABSTRACT We have analyzed the dependence of actin filament sliding movement on the mode of myosin attachment to surfaces. Monoclonal antibodies (mAbs) that bind to three distinct sites were used to tether myosin to nitrocellulose-coated glass. One antibody reacts with an epitope on the regulatory light chain (LC2) located at the head-rod junction. The other two react with sites in the rod domain, one in the S2 region near the S2-LMM hinge, and the other at the C terminus of the myosin rod. This method of attachment provides a means of controlling the flexibility and density of myosin on the surface. Fast skeletal muscle myosin monomers were bound to the surfaces through the specific interaction with these mAbs, and the sliding movement of fluorescently labeled actin filaments was analyzed by video microscopy. Each of these antibodies produced stable myosin-coated surfaces that supported uniform motion of actin over the course of several hours. Attachment of myosin through the anti-S2 and anti-LMM mAbs yielded significantly higher velocities (10 μm/s at 30°C) than attachment through anti-LC2 (4–5 μm/s at 30°C). For each antibody, we observed a characteristic value of the myosin density for the onset of F-actin motion and a second critical density for velocity saturation. The specific mode of attachment influences the velocity of actin filaments and the characteristic surface density needed to support movement.

INTRODUCTION

Molecular motors like myosin play important and multifunctional roles in most higher organisms (Warrick and Spudich, 1987; Spudich, 1989). The robustness of these motors is as remarkable as their efficiency (Cooke, 1986). Despite continuing efforts (Huxley and Simmons, 1971; Eisenberg and Hill, 1985; Pollard, 1987; Huxley, 1990; Huxley, 1992), the precise mechanism of energy transduction and force generation remains elusive. Very accurate knowledge of the static structure of these motor proteins (Holmes et al., 1990; Rayment et al., 1993) is not sufficient to understand their function, and it is difficult to observe their dynamics on a nanometer scale.

The conditions needed to create directed motion in a Brownian physical system have been investigated on theoretical grounds (Ajdari and Prost, 1992; Magnasco, 1993), giving rise to thermodynamic models (Magnasco, 1994; Prost et al., 1994). However, the experimental data remain insufficient to distinguish among these models and to establish their relevance to the case of motor proteins. The energies involved are close to thermal energy, making physical measurements difficult.

Recently, precise measurements of the motion of actin filaments on a few myosin heads and the associated forces were obtained by means of optical tweezers (Finer et al., 1994; Saito et al., 1994). Such experiments give important information on parameters like the step size of the motor, but they address neither the issue of the collective behavior of a large number of myosin molecules in contact with one actin filament, nor global statistical or thermodynamic questions. Thus, macroscopic observation remains an important tool to gain insight into the process of energy transduction. Both approaches, local and global, are complementary.

Global information on the dynamics of motors can be obtained using in vitro motility assays, the observation of actin filaments moving on myosin by means of a fluorescent light microscope. Numerous variations on motility assays have been reported (Kron and Spudich, 1986; Toyoshima et al., 1987; Harada and Yanagida, 1988; Uyeda et al., 1990; Harada et al., 1990; Homsher et al., 1992). They avoid some of the technical problems related to the manipulation and measurement on only a few molecules, but introduce other problems such as: the control of the myosin surface, homogeneity of the distribution of the myosin molecules, defects resulting from nonfunctional myosin heads, and dependence of the measurements on the preparation protocol. Furthermore, the information content of video images is enormous and difficult to manipulate.

In this paper, care has been taken in the preparation of the myosin surface. Myosin is tethered to a nitrocellulose surface via specific attachment to antibodies. Three different mAbs have been used, each one binding to a unique site on myosin. Binding of the mAbs to the nitrocellulose and the subsequent attachment of myosin to the antibody-coated surfaces are characterized by radioimmunoassay. The dependence of the

Received for publication 9 December 1994 and in final form 24 March 1995.

Address reprint requests to Dr. Donald A. Winkelmann, Department of Pathology, UMDNJ-Robert Wood Johnson Medical School, 675 Hoes Lane, Piscataway, NJ 08854. Tel.: 908-235-4759; Fax: 908-235-4825; E-mail: daw@bioimg.umdnj.edu.

Laurent Bourdieu's present address: Institut de Physique, Universite de Strasbourg, Strasbourg, France.

Albrecht Ott's present address: Institut Curie, Section de Physique et Chimie, Paris, France.

Abbreviations used: IgG, immunoglobulin G; mAb, monoclonal antibody; Fab, immunoglobulin antigen-binding fragment; F-actin, filamentous actin; LC2, myosin light chain 2; phR-actin, phalloidin-rhodamine-labeled actin; S2, subfragment-2; LMM, light meromyosin.

0006-3495/95/06/2444/10 $2.00

average velocity of the actin filaments on the buffer components is optimized. The velocity dependence on the surface density of myosin is studied. A critical density for velocity onset and a second critical density for velocity saturation are observed. Above this saturation density, the temperature dependence of the velocity is analyzed. The effect of the mode of attachment on actin filament velocity and on the critical surface densities is discussed. A preliminary report of this work has been presented (Winkelmann et al., 1995).

MATERIALS AND METHODS

Monoclonal antibody preparation and immunochemistry

Monoclonal antibodies 5C3.2, 10F12.3, and 7C10.2 reacting specifically with chicken skeletal muscle myosin heavy and light chains and were prepared and characterized as described previously (Winkelmann et al., 1983; Winkelmann and Lowey, 1986). Myosin isoform specificity was determined by enzyme linked immunoassays and Western; the mAbs 10F12.3 and 7C10.2 react with embryonic, post-hatch, and adult fast skeletal muscle myosin from chickens and do not cross-react with rabbit myosin. In contrast, mAb 5C3.2 reacts with adult fast skeletal muscle myosin from chicken pectoralis and rabbit psoas muscles. The IgG class monoclonal antibodies were purified on protein A-Sepharose (Ey et al., 1978) from ascites fluid obtained by passage of hybridoma lines through CAF1/J mice (Winkelmann et al., 1983). Monoclonal antibodies and myosin were iodinated with $Na^{125}I$ using the chloramine T method (Press, 1981).

Myosin, myosin subfragments, and light chains were prepared from adult White Leghorn chicken pectoralis muscle as described previously (Winkelmann and Lowey, 1986; Winkelmann et al., 1993). Actin was extracted from chicken pectoralis muscle acetone powder, and actin filaments were labeled with phalloidin-rhodamine for motility assays as described previously (Winkelmann et al., 1993). Immunoelectron microscopy of rotary-shadowed molecules was performed as described previously (Winkelmann and Lowey, 1986).

Binding assays

Clean glass coverslips were coated with a thin film of nitrocellulose by evaporation of 10 μl of 0.1% nitrocellulose solution dissolved in amyl acetate (Ernst E. Fullam, Inc., Schenectady, NY) per 254 mm^2 coverslip. The coated coverslips were applied directly to 100- to 150-μl drops of mAb dilution in PBS and incubated for 15 min at 24°C. The antibody-coated surfaces were transferred to drops of PBS supplemented with 1% BSA (BSA/PBS) and blocked for 15 min. The coverslips were transferred to fresh drops of BSA/PBS and may be stored this way in a humidified chamber at 4°C for up to 24 h before use. Binding of ^{125}I-labeled mAb 10F12.3 was used to measure the kinetics and concentration dependence of adsorption to nitrocellulose by drying the coverslips after the second BSA/PBS wash and counting in a gamma counter.

The binding of monovalent Fab antibody fragments to myosin filaments was done as described previously (Winkelmann et al., 1993). The apparent dissociation constants for binding of the Fab fragments to myosin filaments were estimated from the sedimentation data by regression analysis.

Motility assay

Myosin was stored frozen at −130°C in small aliquots (150 μl) at 20–30 mg/ml in HSB (25 mM imidazole, pH 7.6, 0.3 M KCl, 4 mM $MgCl_2$) without loss of activity after rapid freezing with liquid nitrogen (Harada et al., 1990). The frozen myosin aliquots are thawed on ice for about 15 min, then overlaid with 290 μl of fresh HSB and gently mixed by pipetting up and down several times before addition of MgATP (pH 7.0) and 2-mercaptoethanol to 5 mM final concentration each along with 40 μl of 10 mg/ml F-actin (~1/10 the weight of myosin present). The acto-myosin suspension is mixed quickly, transferred to the Beckman (Palo Alto, CA) TLA 100.2 rotor, and the F-actin is pelleted at 90,000 rpm for 21 min (4°C). This procedure pellets all of the actin and 5–10% of the total myosin, including inactive myosin that is no longer dissociated from actin by ATP (dead heads). The clear myosin supernatant is routinely recovered at 8–10 mg/ml and is used immediately for assays. The myosin concentration is determined with the Bio-Rad protein assay (Bio-Rad, Cambridge, MA).

Myosin is diluted in HSB supplemented with 1% BSA (HSB/BSA) to a final concentration of 1–100 μg/ml. The mAb-treated coverslips are incubated on 150-μl drops of the diluted myosin spotted on parafilm in a humidified chamber at 4°C for 2–4 h. The coverslips are washed twice by transferring to 150 μl of HSB/BSA for 5 min/wash, then rinsed twice by transferring to a 150-μl drop of motility buffer (25 mM imidazole, 25 mM KCl, 4 mM $MgCl_2$, 0.2 mM $CaCl_2$, 5 mM 2-mercaptoethanol, 1 mM ATP, pH 7.6) for 30–60 s. The excess motility buffer is wicked off, and the coverslip is mounted on 10 μl of 3 nM phR-actin (see below) in a 11-mm-diameter well of a Teflon-coated glass slide (Cel Line Associates Inc., Newfield, NJ). A ring of Dow-Corning vacuum grease around the well is used to seal the myosin-coated coverslip, forming an incubation chamber with a depth corresponding to the thickness of the Teflon coating (100 μm) and a volume of ~10 μl. The myosin-treated coverslips can be stored at 4°C on a drop of HSB/BSA for several hours before use without adverse effects on activity. The same protocol was used for binding of ^{125}I-labeled myosin to antibody-coated surfaces, but after the motility buffer wash, the coverslips were dried and counted in a gamma counter.

Phalloidin-rhodamine-labeled actin was diluted to 3–6 nM with motility buffer supplemented with 0.5% 2-mercaptoethanol, 0.1 mg/ml glucose oxidase, 0.018 mg/ml catalase, and 2.3 mg/ml glucose to remove oxygen (Kishino and Yanagida, 1988). In most assays, the MgATP concentration was increased to 7.5 mM and 0.5% methyl cellulose (1500 centipoises/2% aqueous solution; Sigma Chemical Co., St. Louis, MO) was also added. This chamber was observed with a 63× or 100× Plan Apochromat objective on a Zeiss microscope (Carl Zeiss Inc., Thornwood, NY) equipped with epifluorescence optics illuminated with a 75 W xenon or 50 W mercury light source and rhodamine filter set. Images were projected with a 4× TV tube onto the photocathode of a microchannel plate image intensifier (Hamamatsu Photonics, Bridgewater, NJ) optically coupled to a newvicon video camera and recorded with a VHS or SVHS video recorder. Movement of actin filaments in the sealed chamber can be observed for >2 h; however, measurements were taken within 30 min of slide preparation. Video segments of at least 5 min were recorded from several fields for each assay condition.

Motion analysis

Video images of movement sequences were captured and digitized using an Androx (Boston, MA) frame grabber on a IRIS-4D70GT workstation (Silicon Graphics Inc., Mountain View, CA). A portion of individual video frames corresponding to a 256×256 pixel array was digitized from video tape records at sampling rates corresponding to 3–15 frames/s. The digitized images were sampled on a raster of 0.14 μm/pixel that was calibrated with an slide micrometer. The image acquisition rate was variable and selected to match the velocity of the actin filaments such that the spatial resolution between frames for the most rapidly moving filaments was about 0.4 μm/frame. Segments of 5–20 s duration and containing 64–128 individual digital frames correspond to a video sequence. The tracks of 30–50 actin filaments with uninterrupted motion over a distance >5 μm were selected from 6–10 different locations on the sealed chamber. The velocity of the filaments was measured using an interactive tracking program on the digitized video sequences by tracking the leading edge of moving filaments. Mean value and SD of the velocities are presented. Stationary filaments and filaments that moved <3 μm were not included in the measurements.

RESULTS

Characterization of the surfaces

We have undertaken an analysis of the dependence of actin filament sliding movement on the mode of myosin

attachment to surfaces. To accomplish this, monoclonal antibodies (mAbs) that bind to three distinct sites have been used to tether myosin to nitrocellulose-coated glass. Rotary-shadowed electron micrographs of the three mAbs reveal the location of the attachment sites on myosin (Fig. 1). One antibody reacts with an epitope on the regulatory light chain (LC2) between residues 17 and 51 (anti-LC2, 7C10.2) (Winkelmann and Lowey, 1986). This mAb binds to the B helix of the divalent cation-binding EF-hand on LC2 and is located on subfragment-1 at the furthest point from the actin-binding surface (Rayment et al., 1993). Fab fragments of this antibody have no effect on myosin ATPase activity or sliding movement of actin filaments in motility assays (Winkelmann et al., 1993). The other two mAbs react with sites in the rod domain, one in the S2 region 42 nm from the head-rod junction near the S2-LMM hinge (anti-S2, 10F12.3), and the other at the C terminus of the myosin rod (anti-LMM, 5C3.2). Each of these antibodies binds tightly and specifically to myosin. Two anti-S2 or anti-LMM antibodies frequently bind to opposing sides of the rod (Fig. 1). This type of binding is also observed with the anti-LC2 antibody (not shown). The characteristics of the mAbs and the location of the binding sites on myosin are summarized in Table 1. As suggested by the images, these antibodies provide increasing flexibility in the mode of attachment of myosin to surfaces.

The concentration dependence and kinetics for nonspecific adsorption of mAbs to nitrocellulose-coated glass are presented in Fig. 2. Saturation of the surface with antibody is complete in 10 min using an antibody concentration of 180 μg/ml and approaches 11,000 mol/μm^2. Assuming formation of a monolayer on the nitrocellulose, this density corresponds to a surface of close packed molecules with an average spacing of 10–12 nm. Each of these mAbs has been produced in high yield (2–5 mg/ml) in ascites fluid by passage of the cell lines in mice, and the myosin-specific IgG antibody isolated >90% pure (not shown). Therefore, these surfaces contain a dense array of myosin specific binding sites. Routinely, 150 μg/ml and 15-min incubations were used to prepare antibody-coated nitrocellulose surfaces for all three antibodies. Nonspecific binding sites that remained were blocked with 1% BSA in PBS- and antibody-coated surfaces were stable for 24 h when stored on this buffer at 4°C.

The antibody-coated surfaces were incubated with monomeric ^{125}I-labeled myosin diluted in HSB/BSA at 4°C to measure the binding characteristics of the surfaces (Fig. 3). Binding saturates with increasing myosin concentration, and the plateau value differs for the three different antibodies. This probably reflects variation in the extent of molecular crowding at the surface that is dependent on the location of the epitope on myosin. The kinetics of binding is quite slow, achieving 90% saturation of binding in 3 h at 10 μg/ml myosin (not shown). The reproducibility of the binding assay is very good, and the surfaces are stable once myosin is bound. Fig. 3 *B* is a blow-up of the low concentration range over which most motility assays are done. This corresponds to a myosin surface density of 10–1000 mol/μm^2. The myosin surface density can be modified in a controlled way by varying the concentration of myosin in the solution.

TABLE 1 Summary of mAb specificity

mAb Clone designation	Immunoglobulin isotype	Myosin fragment specificity	Distance from head-rod junction
7C10.2	IgG_1	$LC2_{17-51}$	0 nm
10F12.3	IgG_1	S2	42 nm
5C3.2	IgG_{2b}	LMM	150 nm

Table 2 summarizes the apparent dissociation constants (K_d) for myosin binding to each of the antibody surfaces derived from the binding isotherms (Fig. 3). The binding constants for Fab fragments of two of the antibodies were determined in a sedimentation assay with myosin filaments and are compared in this table. For both of these antibodies, the dissociation constants for the monovalent Fab fragments is roughly the square of the K'_d for the surface interaction. This is evidence of a bivalent interaction of myosin with the antibody surface and explains the stability of the surfaces once myosin is bound. A dense myosin surface (600–1000 mol/μm^2) is obtained using lower concentrations of myosin than in most other assay protocols because of the high affinity of these specific antibodies.

Actin filament motion on antibody-tethered myosin

At sufficiently high surface densities (600–1000 mol/μm^2), myosin tethered by each of the antibodies supported rapid sliding motion of actin filaments over the course of several hours. The persistence of the motion results from the stable attachment of the myosin. The actin filaments move smoothly onto the myosin surface from bulk solution and often transit over distances of several hundred micrometers. This suggests a homogeneous deposition of myosin and little inactivation of the myosin during preparation of the surface. There are several significant improvements in the quality of

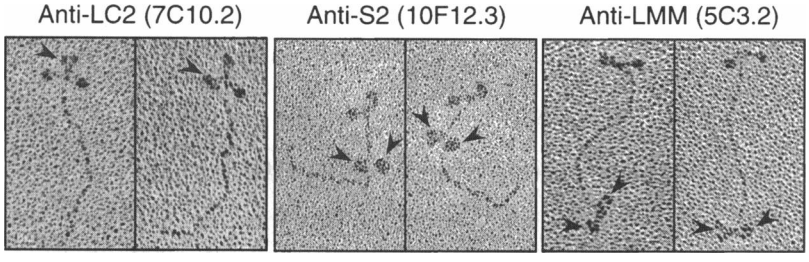

FIGURE 1 mAbs that bind to three distinct sites were used to tether myosin to nitrocellulose-coated glass. Rotary-shadowed electron microscopic images of antibody-myosin complexes show the location of the antibody binding sites on myosin. The arrowheads identify the IgG antibody molecules bound to myosin. Replicas were prepared and photographed as described previously (Winkelmann et al., 1983; Winkelmann and Lowey, 1986).

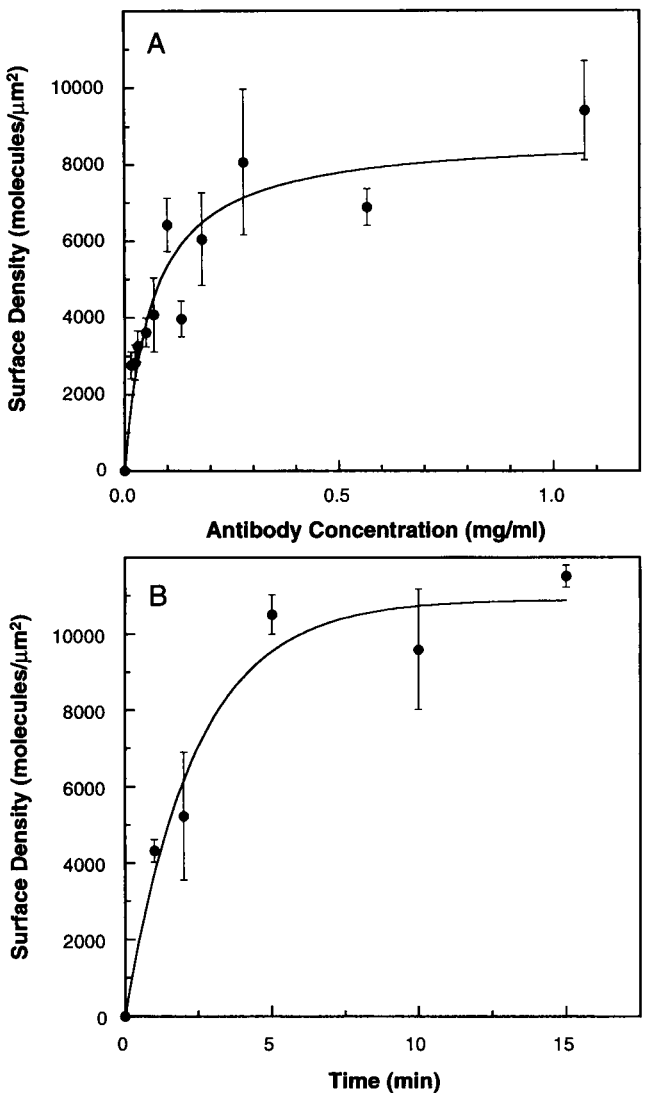

FIGURE 2 The antibody concentration dependence and kinetics for nonspecific adsorption of mAb to nitrocellulose-coated glass. (*A*) Glass coverslips were coated with nitrocellulose as described in Materials and Methods and then incubated with increasing concentrations of ^{125}I-labeled anti-S2 mAb 10F12.3 for 2 min at 24°C. The coverslips were washed, dried, and bound radioactivity-assayed. Binding of the antibody saturates at a density of approximately 8000 mol/μm^2 at concentrations above 0.3 mg/ml mAb. (*B*) The time course of binding of 0.18 μg/ml ^{125}I-labeled mAb 10F12.3 indicates that saturation of the surface is complete in ~10 min and approaches 11,000 mol/μm^2 bound mAb. Assuming formation of a monolayer on the nitrocellulose, this density would correspond to a surface of close packed mAb with an average spacing between molecules of 10–12 nm. The line in *A* is the fit of the general binding equation: $B = B_{max}[mAb]/(K_d + [mAb])$, to the data. The line in *B* is a fit of the exponential rate expression: $B = B_{max}(1 - e^{-kt})$, to the data.

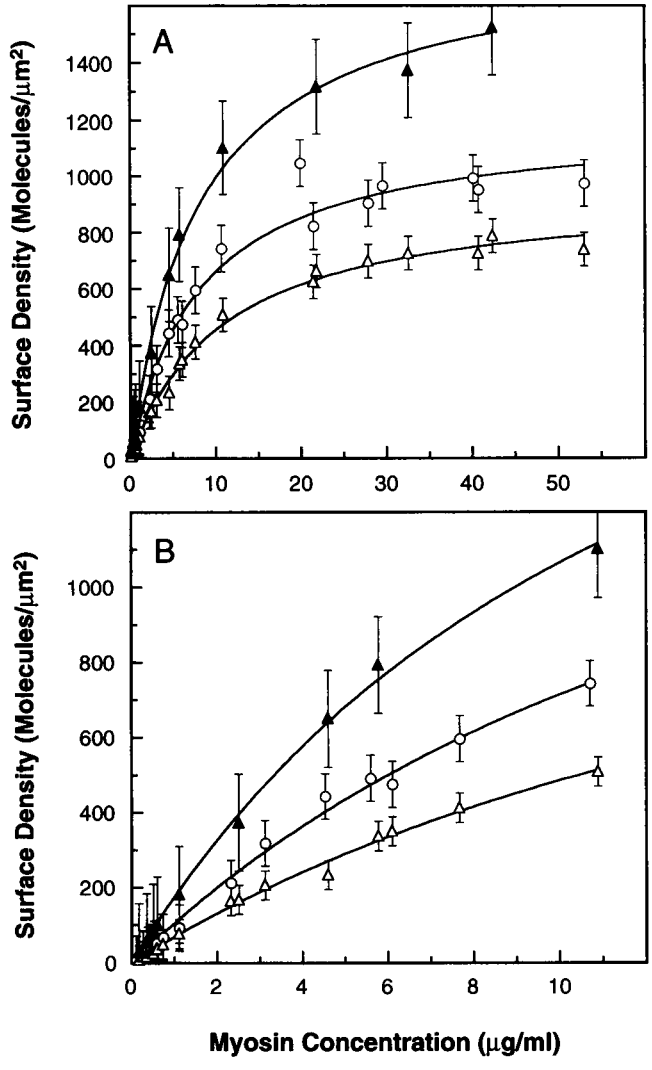

FIGURE 3 Myosin-binding capacity and surface density on antibody-coated coverslips. Antibody capture surfaces were prepared with mAbs anti-LC2 (7C10.2), anti-S2 (10F12.3), and anti-LMM (5C3.2) using freshly prepared nitrocellulose-coated glass coverslips incubated with 0.15 mg/ml of each mAb for 15 min at 24°C. (*A*) The binding of ^{125}I-labeled myosin was measured after incubation with anti-LC2 (△)-, anti-S2 (○)-, or anti-LMM (▲)-coated surfaces for 2 h at 4°C. (*B*) Myosin surface density over the concentration range 0–12 μg/ml for the three mAbs. ^{125}I-labeled myosin was diluted in HSB/BSA, and the concentration of the myosin dilution was determined by counting a small aliquot. Bound radioactivity was measured by counting dried coverslips after washing 3 times with HSB/BSA and once with motility buffer. Nonspecific binding of myosin to BSA-blocked coverslips was subtracted from each assay point and represented <2% of the bound radioactivity over the entire concentration range. The lines are a fit of the general binding equation to the data as in Fig. 2.

motion on the antibody-tethered myosin surfaces compared with other methods that we have used, including myosin filaments adsorbed to glass, monomeric myosin adsorbed to silicon-treated glass, or nitrocellulose films.

The improvements are illustrated by the accumulation of actin filament tracks in a single field over 8 min of observation (Fig. 4). Each line corresponds to the track followed by a single filament as it transits over the surface of myosin. Individual tracks are apparent at short times (90 s), but become difficult to discern after accumulation over 8 min, when the entire field is filled with the intermingled tracks of hundreds of filaments. Immobilized filaments give rise to bright spots. There are relatively few surface defects resulting in pinned or immobilized filaments. This results in more homogeneous motion of actin filaments and an abundance of movement trajectories. The complete coverage of the field with tracks suggests that the distribution of myosin molecules on the surface is uniform. The dispersion of actin

TABLE 2 Binding constants of mAbs

mAb	Specificity	Monovalent binding assay K_d	Surface assay K_d'
7C10.2	anti-LC2	400 nM	20.9 nM
10F12.3	anti-S2	170 nM	15.8 nM
5C3.2	anti-LMM	ND*	15.3 nM

*ND, not determined.

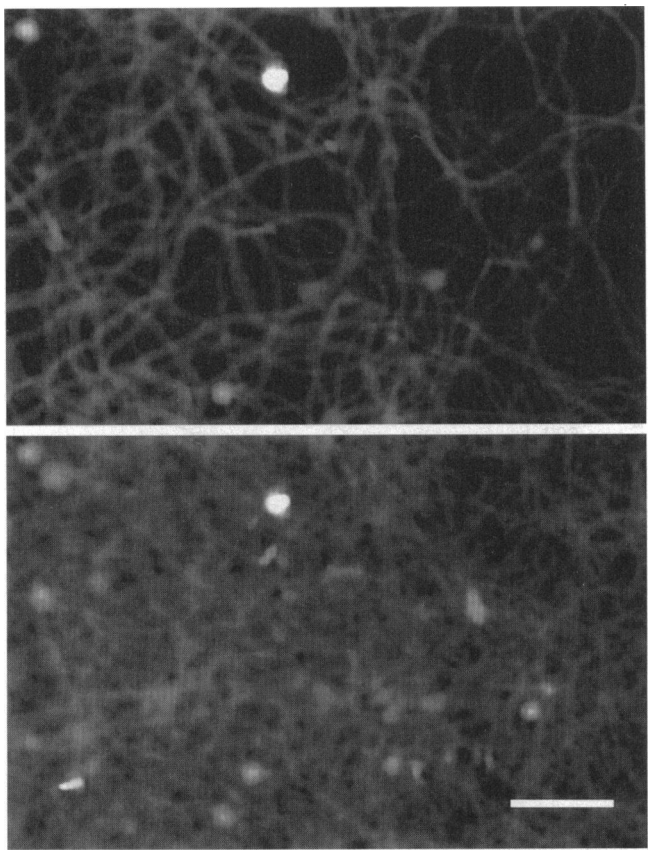

FIGURE 4 Summation of actin filament tracks over a saturated myosin-coated surface. Myosin was tethered through the anti-S2 mAb (10F12.3), and actin filament motion was recorded at 25°C. The tracks for filaments transiting through the field of view were determined with a computer tracking program over a period of 8 min. (*top*) The summation of tracks formed over a period of 90 s of observation is presented. Note the uniform distribution of tracks and the limited number of pinned filaments. (*bottom*) The summation of tracks in the same field after 8 min of observation. These images demonstrate the uniformity of the surface distribution of myosin and the low number of point defects that trap and hold actin filaments. New actin filaments are transiting continuously through the field, making possible the observation of the same area for long periods without concern for photobleaching. Bar is 10 μm long.

filament velocities was typically on the order of 10–15% for actively moving filaments in any given sample. No variation of this average speed with time was detected, hence the degradation of the motor during observation can be neglected. Additionally, velocity measurements are highly reproducible between different samples measured under the same conditions. These results contrast with our experience using other methods of surface preparation.

One difference that was immediately apparent between the myosin surfaces prepared with the three mAbs is that the average actin filament velocity produced by the anti-LC2-tethered myosin was lower than that produced by myosin tethered to the anti-LMM and anti-S2 mAbs. Attachment of myosin through either the anti-S2 or anti-LMM mAbs yielded an average velocity of 10 μm/s at 30°C, whereas attachment through anti-LC2 produced a lower velocity of 4–5 μm/s. Attachment of myosin via anti-LC2 also stimulates actin filament breakage above that seen with the other modes of attachment, rapidly producing short filaments 1–4 μm long. The decreased velocity and increased filament breakage suggest that reduced flexibility increases surface friction. Toyoshima et al. (1987) observed a similar decreased velocity with myosin subfragment-1 bound directly to nitrocellulose as compared with HMM and suggested that it arises from increased restraining force due to unfavorably oriented heads. Other differences in actin filament motion among the different modes of attachment are discussed below.

Optimization of the assay conditions

Myosin tethered at high surface densities (>800 mol/μm^2) to the anti-S2 mAb was used to define the experimental conditions needed to optimize the velocity of F-actin motion. The pH and ionic strength dependence of the assay are essentially identical to those reported for rabbit skeletal muscle myosin (Homsher et al., 1992). Velocities are higher under slightly alkaline conditions and moderate ionic strength (40–80 mM); throughout we have used a pH of 7.6 and an ionic strength of 65 mM. Maximum velocity is obtained for concentrations of magnesium at or slightly above a 1:1 ratio between magnesium and ATP. The velocity of actin filaments as a function of MgATP concentration for different temperatures is shown in Fig. 5 *A*. At each temperature, the curve shows a maximum at about 7.5 mM MgATP. Above this concentration, there is a decrease in adherence of the filaments to the surface. At 15 mM MgATP, the filaments move smoothly on the surface for a few seconds and then leave it; above 20 mM MgATP, the filaments do not adhere. However, in this experiment, the total ionic strength was not held constant and was varied over the range 44–105 mM with increasing MgATP. The rise in ionic strength contributes to decreased localization of the filaments near the surface at higher MgATP concentrations.

Measurement of the variation of the average speed as a function of MgATP concentration but at constant ionic strength (65 mM) is shown in Fig. 5 *B*. The speed reaches a plateau at a maximum value (V_{max}), in agreement with previous reports (Homsher et al., 1992; Kron and Spudich, 1986; Umemoto and Sellers, 1990). The K_m is on the order of 0.2 $\pm$ 0.15 mM MgATP, in agreement with published values (Homsher et al., 1992; Kron and Spudich, 1986; Tesi et al., 1991); however, there is a large uncertainty in K_m because we have focused on higher MgATP concentrations. There is a definite saturation of the velocity with increasing MgATP at constant ionic strength.

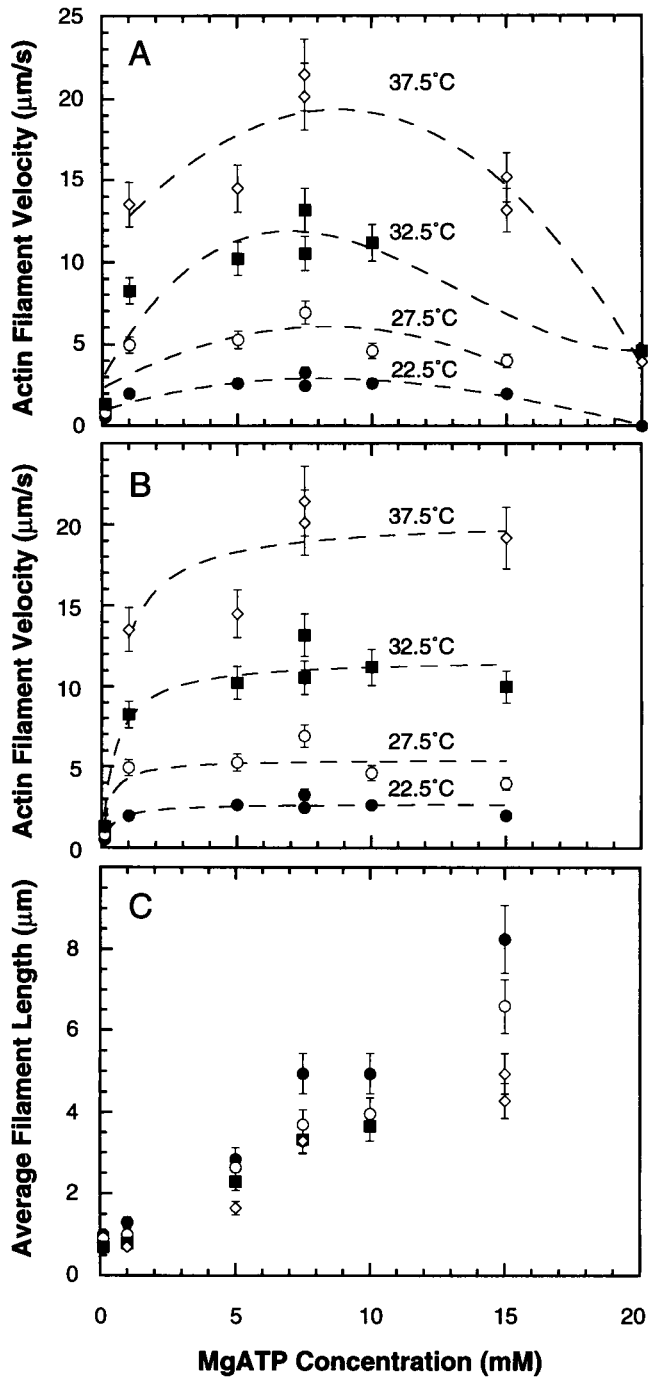

FIGURE 5 Average velocity of actin filaments as a function of the MgATP concentration for different temperatures (● 22.5°C; ○ 27.5°C; ■ 32.5°C; □ 37.5°C). The surface concentration of myosin is 1000 mol/μm^2. (*A*) The ionic strength of the buffer solution is not kept constant, and filament speed decreases at large MgATP concentration. The dotted lines are guides for the eyes. (*B*) The ionic strength is held constant by varying the KCl concentration of the buffer solution (65 mM); the filaments velocity saturates. The dotted lines are a fit to the experimental points, using the following equation: $V = V_0/(1 + K_m/[MgATP])$. (*C*) The average of the distribution of filament length as a function of MgATP concentration for different temperatures (● 22.5°C; ○ 27.5°C; ■ 32.5°C; □ 37.5°C).

Decreased actin filament velocity and increased filament breakage can be achieved by lowering the ATP concentration. This decreases the rate of myosin dissociation from actin so that tightly bound myosin heads begin to form that resist the action of actively cycling heads (Harada et al., 1990). Fig. 5 *C* shows the average of the length distribution of actin filaments as a function of MgATP concentration for different temperatures. At low MgATP concentrations, the filaments are broken, regardless of temperature. New longer filaments arriving from the chamber volume onto the surface break after a few seconds. This suggests a strong friction between the substrate and the filaments resulting from insufficient MgATP. This friction is reduced at higher MgATP concentrations, resulting in longer filaments. In addition, one observes a global decrease of the average filament length as the temperature increases. It is surprising that MgATP has an effect on filament length well above the concentration needed to saturate the velocity of filament motion.

Average velocity versus myosin surface density

One of the most important factors in determining the velocity of actin filament motion is the surface density of myosin molecules (σ). The myosin surface density is readily varied on the antibody-coated nitrocellulose by adjusting the myosin concentration (Fig. 3). The effect of the variation of surface density and mode of attachment on the average velocity of actin filament motion is presented in Fig. 6. To increase

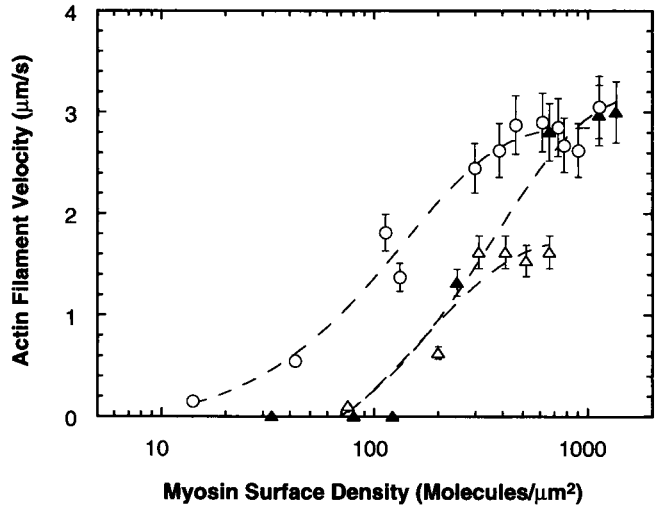

FIGURE 6 Average actin filament velocity as a function of the myosin surface density and the mode of attachment. For each antibody (anti-LC2 (7C10.2, δ), anti-S2 (10F12.3,○), or anti-LMM (5C3.2, ▲)) a characteristic myosin density σ_{onset} was observed below which sliding movement was no longer supported. Above a second characteristic density σ_{sat}, velocity saturates at a value V_{sat}, which is the same for the anti-LMM and anti-S2 antibodies and 50% slower for anti-LC2. These data were collected at 23°C, and data points correspond to the average velocity V_{max} of long filaments (see text) measured during the period of directed motion. The lines correspond to a fit of the equation $V_{max}(\sigma) = V_{sat}(1 - \exp(-m(\sigma - \sigma_{onset})))$ to the experimental data. The same fit was used for each antibody. Only in the case of 10F12.3 are there enough points between σ_{onset} and σ_{sat} to determine accurately the shape of the experimental curve.

the adherence of F-actin at low myosin densities, methyl cellulose (0.5%) was included in these assays (Uyeda et al., 1990). The actin filament velocity has a complex dependence on myosin surface density, actin filament length, and mode of attachment. No motion is detected below a myosin surface density required for the onset of motion (σ_{onset}), and this density is dependent on the mode of attachment; σ_{onset} varies between 10 and 70 moleμm^2 for the three different modes of tethering myosin to surfaces. Above a critical surface density (σ_{sat} = 300–600 mol/μm^2) the velocity saturates to a value V_{sat} independent of the actin filament length. The average velocity is well defined at that density for both long and short actin filaments. In the intermediate range of surface densities where $\sigma_{onset} < \sigma < \sigma_{sat}$, the actin filament velocity depends on the filament length, for each σ it saturates for the longest filaments to a value V_{max}. The velocities plotted in Fig. 6 correspond to V_{max}, which is an increasing function of σ.

These results are consistent with previously published data (Uyeda et al., 1990). However, what has not been noted previously is that the saturation velocity (V_{sat}) and the characteristic densities are dependent on the mode of attachment of myosin to surfaces. The value of V_{sat} is the same for myosin tethered via the anti-S2 and anti-LMM mAbs and 50% slower for the anti-LC2-tethered myosin. The transition between the onset of motion and velocity saturation extends over a much larger range of surfaces densities for myosin attached via the anti-S2 mAb (10F12.3), and the overall quality of motion with this mode of attachment is the best. The surface density of myosin required for the onset of motion and for velocity saturation for each of the three modes of attachment is summarized in Table 3.

The nature of the motion itself is dependent on the surface density. At high surface density ($\sigma \geq \sigma_{sat}$), the smooth motion of the filaments is interrupted only occasionally by short pinning events, resulting in stalls. The motion is more irregular and the pinning times are longer below σ_{sat}. The shorter filaments move more irregularly, and at very low myosin surface densities (σ < 200 mol/μm^2), the motion of filaments shorter than 1 μm becomes undirected and Brownian-like.

Average velocity versus temperature

The influence of temperature (10–35°C) on filament velocity was studied for each of the modes of attachment at myosin surface densities of 800–1000 mol/μm^2 (Fig. 7). Surfaces prepared with anti-S2 (10F12.3) and anti-LMM (5C3.2) show the same unusual temperature dependence in which two regimes can be distinguished. At lower temperatures (below 17.5°C), the velocity increases very rapidly with the temperature from 0.15 μm/s at 10°C to ~1 μm/s at 17.5°C. Above 17.5°C the velocity increases more slowly, reaching 15 μm/s at 35°C. In the higher temperature regime, the logarithm of the velocity has a linear dependence with the inverse of the absolute temperature and a slope of 40 k_BT. Attachment of myosin via anti-LC2 (7C10.2) leads to significantly smaller velocities at all temperatures above 10°C with the same apparent slope (40 k_BT). The value of 40 k_BT (98 kJ/mole) is consistent with previous reports (Homsher et al., 1992) and with the activation energy of the actin activated myosin ATPase, obtained by direct measurement of the released phosphate (Tesi et al., 1991).

DISCUSSION

We have presented a protocol for in vitro motility assays, based on tethering myosin to surfaces through the specific attachment to mAbs. This method improves the quality of the actin filament motion by reducing the density of surface defects. The precise mode of myosin attachment influences motion in two significant ways: the average velocity is reduced when the motor domain is fixed too close to the supporting surface, and the myosin density for the onset of actin filament motion is dependent on the flexibility of attachment. The best overall motion is achieved when the mode of attachment most closely approximates that of myosin in muscle thick filaments, i.e., tethered through the anti-S2 mAb with much of the S2 region of the rod free.

The protocol described in this paper improves significantly the quality and the reproducibility of the assay. The binding characteristics of the nitrocellulose were characterized carefully so that saturated surfaces containing an excess of antibody are routinely produced. The choice of antibodies was restricted to those that favored bivalent interactions with

TABLE 3 Dependence of actin filament velocity on myosin surface density

Antibody	V_{sat} @ 23°C (μm/s)	σ_{onset} (mol/μm^2)	d_{onset} (μm)	σ_{sat} (mol/μm^2)	d_{sat} (μm)	w (μm)	πw^2 (μm^2/mol)	$2/3\pi w^3$ (μm^3/mol)
anti-LC2 (7C10.2)	1.5	70	0.135	300	0.065	0.020	1.26E-03	1.68E-05
anti-S2 (10F12.3)	2.9	10	0.357	400	0.056	0.062	1.21E-02	4.99E-04
anti-LMM (5C3.2)	3.2	70	0.135	600	0.046	0.170	9.08E-02	1.03E-02

$$\nu = \nu_{max}(1 - \exp(-m(\sigma - \sigma_{onset})))$$

Values of V_{sat}, ς_{onset}, and ς_{sat} are obtained from the fit of the equation (shown below the table) to the data in Fig. 6. These data were collected at 23°C. The reaching distance, w, is estimated as the distance from the location of the antibody attachment site on myosin to the actin-binding surface with an additional 10 nm added for the height of the flexible Fab arms of the IgG antibody above the nitrocellulose surface. The average spacing between molecules, d, is estimated as: $d = 2(\varsigma\pi)^{-1/2}$. The area and hemispherical volume that are accessible to the myosin heads for each of the modes of attachment are calculated.

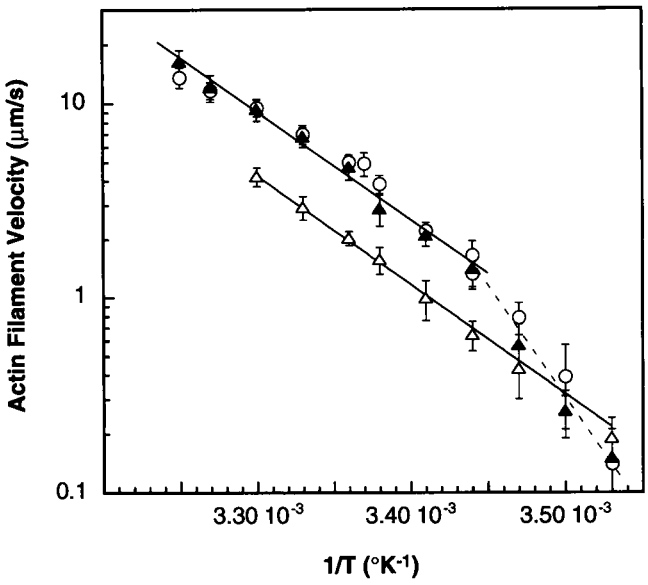

FIGURE 7 The average F-actin velocity as a function of the inverse temperature for myosin tethered via the three antibodies (△ 7C10.2; ○ 10F12.3, ▲ 5C3.2). For 7C10.2, the solid line fit follows equation $V = A \exp(-E/k_BT)$, where $E = 40k_BT$. For 10F12.3 and 5C3.2, two regimes appear with a transition at 17.5°C: in the high temperature regime, the solid line is a fit following the Arrhenius behavior, with $E = 40k_BT$. The dotted line is an approximation to illustrate the break in the temperature dependence for attachment through the rod at temperatures below 17.5°C.

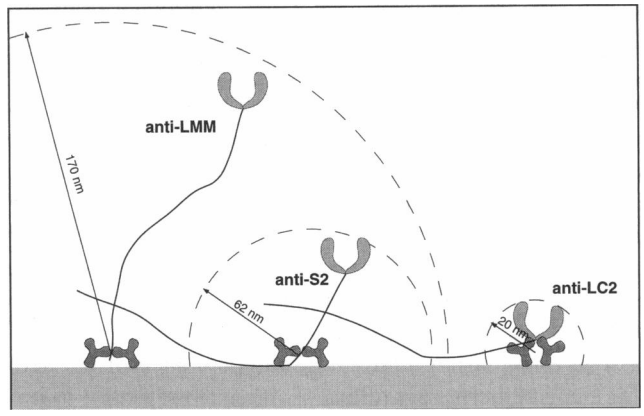

FIGURE 8 Schematic diagram depicting the ideal disposition of myosin monomers tethered to the surface by the three mAbs. Each myosin is shown simultaneously bound by two Fab arms of the IgG mAb. The radius vector depicts the reaching distance, w, from the attachment point to the actin-binding surface on the myosin head.

myosin so stable surfaces would result, and mAbs were used that could be isolated at least 90% pure to increase the density of active attachment sites on the surface. With the characteristics of the binding surface established, the mode of attachment of myosin could be controlled and the myosin surface density varied and measured. We have compared this method of myosin surface preparation with several other methods, such as direct binding of myosin filaments to glass and nitrocellulose-coated glass (Kron and Spudich, 1986) and binding monomeric myosin to nitrocellulose-treated or siliconized glass surfaces (Toyoshima et al., 1987, 1990; Harada et al., 1990). None of these methods have produced the uniformity of motion or reproducibility that have resulted from using mAb-coated nitrocellulose surfaces.

Development of this method of tethering myosin enabled us to vary the geometry of the attachment of the motor and test the influence of surface geometry on the motor efficiency. This is illustrated in Fig. 8. Differences are seen in the motion obtained using the three antibodies. Reducing the flexibility of the myosin motor domains by attachment with anti-LC2 (7C10.2) increases the surface friction, induces filament breakage, and reduces the average filament velocity. Conversely, increasing the flexibility of the attachment by tethering myosin through the S2 and LMM regions of the rod results in an increase in filament velocity and filament length; both are consistent with reduced friction. When the surface is saturated with myosin, motion is observed even when the myosin molecule is attached at the C terminus of the rod, placing the motor domains as much as 170 nm from the surface attachment point (Fig. 3).

The mode of attachment affects the characteristic myosin surface densities for the onset of motion and velocity saturation. In a simple model, an actin filament moving on a myosin surface interacts with myosin heads located in a bandwidth w, where w corresponds to the characteristic distance over which a myosin molecule can reach an actin filament (Uyeda et al., 1990; Duke et al., 1994). The reaching distance, w, is a priori directly proportional to the distance between the motor domain and the attachment site of the myosin on the surface. Estimates of w for myosin tethered to the three mAbs are given in Table 3. In such a model, it follows that as w increases σ_{onset} should decrease. The results summarized in Table 3 indicate that this is the pattern for myosin tethered via the anti-LC2 and anti-S2 mAbs, but not for myosin attached via the anti-LMM antibody. This may result from a decrease in efficiency of the motor domain tethered 170 nm from the surface when the myosin density is decreased. Molecules of myosin that may be able to reach F-actin may not interact effectively to contribute to motion. The longer reaching distance imposed by attachment through anti-LMM also results in a 20-fold larger volume explored by the myosin heads tethered in this manner compared with the volume explored for the reach imposed by the anti-S2 mAb (Table 3). This may contribute to a decrease in the efficiency of interaction with F-actin for this mode of attachment. Velocity measurements alone are not sufficient to understand these observations; they need to be complemented by a study of the load dependence of the velocity for the three modes of attachment.

Movement of F-actin along myosin-coated surfaces presupposes that the filaments are localized close to the myosin heads. The dependence of filament velocity on ionic strength and MgATP concentration indicates that motion requires simultaneously localization of the filaments near the myosin surface and minimization of the friction exerted by slowly detaching heads at low MgATP that break the filaments. Increasing the MgATP concentration leads to a decrease in

the surface friction, higher velocities, and longer filaments. However, if the ionic strength is not held constant, velocity is reduced at high MgATP because filaments adhere less to the myosin-coated surface. The addition of 0.5% methyl cellulose in the motility buffer, which in effect reduces the vertical dimension and increases the actin-myosin cross section, has the same effect as reducing the ionic strength; the velocity increases, then saturates with increasing MgATP concentration. Thus, the sticking force is the relevant parameter, not the absolute value of the ionic strength.

There is a strong temperature dependence of the actin filament velocity regardless of the antibody used to prepare the surfaces at saturation of myosin. More precisely, the absolute value of the velocity is dependent on the exact surface preparation, whereas the thermodynamics of the motion is not. The slopes of the Arrhenius plots over the range 17.5–37.5°C are on the order of 40 k_BT (98 kJ mol^{-1}). Below 17.5°C there is an abrupt break in the temperature dependence of the velocity for filaments moving on myosin attached via the anti-S2 and anti-LMM mAbs, but not via anti-LC2 (Fig. 7). A break point in the Arrhenius plot in this temperature range has been observed previously (Sheetz et al., 1984; Homsher et al., 1992). The interpretation of this break is not known. It may reflect a change in the uniformity of the filament motion that is masked by measurement of average velocities. An analysis of the distribution of instantaneous velocities along filament trajectories is in progress and should help clarify this point.

The antibody capture approach has been used before to isolate specific myosin isoforms from a mixture and then measure the motile activity of the isolated myosin (Hynes et al., 1987; Sellers et al., 1993; Cuda et al., 1993; Lowey et al., 1993). Our data demonstrate the sensitivity of this approach for binding myosin from dilute mixtures (Fig. 3), but they also emphasize a caveat of using this method. Because the velocity is influenced by both the mode of attachment and the myosin surface density, careful selection of the antibody and characterization of the surfaces are necessary for interpreting velocity differences between myosin isoforms isolated in this way.

T. Duke, L. Faucheux, P. Kaplan, S. Leibler, and M. Magnasco have contributed greatly through comments, discussions, and advice.
This work is supported by National Institutes of Health grant R01-AR38454 (D.A.W.) and National Science Foundation grant PHY-9408905 (A.L.).

REFERENCES

Ajdari, A., and J. Prost 1992. Drift induced by a spatial periodic potential of low symmetry: pulsed electrophoresis. *C. R. Acad. Sci. Paris II.* 315: 1635–1639.

Cooke, R. 1986. The mechanism of muscle contraction. *CRC Crit. Rev. Biochem.* 21:53–118.

Cuda, G., L. Fananapazir, W. S. Zhu, J. R. Sellers, and N. D. Epstein. 1993. Skeletal muscle expression and abnormal function of beta-myosin in hypertrophic cardiomyopathy. *J. Clin. Invest.* 91:2861–2865.

Duke, T., T. E. Holy, and S. Leibler. 1995. Gliding assays for motor proteins: a theoretical analysis. *Phys. Rev. Lett.* 74:330–333.

Eisenberg, E., and T. L. Hill. 1985. Muscle contraction and free energy transduction in biological systems. *Science.* 227:999–1006.

Ey, P. L., S. J. Prowse, and C. R. Jenkins. 1978. Isolation of pure IgG_1, IgG_{2a} and IgG_{2b} immunoglobulins from mouse serum using protein A-sepharose. *Immunochemistry.* 15:429–436.

Finer, J. T., R. M. Simmons, and J. A. Spudich. 1994. Single myosin molecule mechanics: piconewton forces and nanometre steps. *Nature.* 368: 113–119.

Harada, Y., and T. Yanagida. 1988. Direct observation of molecular motility by light microscopy. *Cell. Motil. Cytoskel.* 10:71–76.

Harada, Y., K. Sakurada, T. Aoki, D. D. Thomas, and T. Yanagida. 1990. Mechanochemical coupling in actomyosin energy transduction studied by in vitro movement assay. *J. Mol. Biol.* 216:49–68.

Holmes, K. C., D. Popp, W. Gebhard, and W. Kabsch. 1990. Atomic model of the actin filament. *Nature.* 347:44–49.

Homsher, E., F. Wang, and J. R. Sellers. 1992. Factors affecting movement of F-actin filaments propelled by skeletal muscle heavy meromyosin. *Am. J. Physiol.* 262:714–723.

Huxley, A. 1992. A fine time for contractual alterations. *Nature.* 357:110.

Huxley, A. F., and R. M. Simmons. 1971. Proposed mechanism of force generation in striated muscle. *Nature.* 223:533–538.

Huxley, H. E. 1990. Sliding filaments and molecular motile systems. *J. Biol. Chem.* 265:8347–8350.

Hynes, T. R., S. M. Block, B. T. White, and J. A. Spudich. 1987. Movement of myosin fragments in vitro: domains involved in force production. *Cell.* 48:953–963.

Kishino, A., and T. Yanagida. 1988. Force measurements by micromanipulation of a single actin filament by glass needles. *Nature.* 334:74–76.

Kron, S., and J. A. Spudich. 1986. Fluorescent actin filaments move on myosin fixed to a glass surface. *Proc. Natl. Acad. Sci. USA.* 83: 6272–6276.

Lowey, S., G. S. Waller, and K. M. Trybus. 1993. Function of skeletal muscle myosin heavy and light chain isoforms by an in vitro motility assay. *J. Biol. Chem.* 266:20414–20418.

Magnasco, M. M. 1993. Forced thermal ratchets. *Phys. Rev. Lett.* 71: 1477–1481.

Magnasco, M. M. 1994. Molecular combustion motors. *Phys. Rev. Lett.* 72:2656.

Pollard, T. D. 1987. The myosin crossbridge problem. *Cell.* 48:909–910.

Press, J. L. 1981. The CBA/N defect defines two classes of T cell-dependent antigens. *J. Immunol.* 126:1234–1240.

Prost, J., J.-F. Chauvin, L. Peliti, and A. Ajdari. 1994. Asymmetric pumping of particles. *Phys. Rev. Lett.* 72:2652*a*. (Abstr.)

Rayment, I., W. R. Rypniewski, K. Schmidt-Base, R. Smith, D. R. Tomchick, M. M. Benning, D. A. Winkelmann, G. Wesenberg, H. M. Holden. 1993. The three-dimensional structure of a molecular motor, myosin subfragment-1. *Science.* 261:50–58.

Saito, K., T. Aoki, T. Aoki, and T. Yanagida. 1994. Movement of single myosin filaments and myosin step size on actin filament suspended in solution by a laser trap. *Biophys. J.* 66:769–777.

Sellers, J. R., G. Cuda, F. Wang, and E. Homsher. 1993. Myosin-specific adapations of the motility assay. *Methods Cell Biol.* 39:23–50.

Sheetz, M. P., R. Chasan, and J. A. Spudich. 1984. ATP-dependent movement of myosin in vitro: characterization of a quantitative assay. *J. Cell Biol.* 99:1867–1871.

Spudich, J. A. 1989. In pursuit of myosin function. *Cell Regul.* 1:1–11.

Tesi, C., K. Kitagishi, F. Travers, and T. Barman. 1991. Cryoenzymatic studies on actomyosin ATPase: kinetic evidence for communications between the actin and ATP binding sites on myosin. *Biochemistry.* 30: 4061–4067.

Toyoshima, Y. Y., S. J. Kron, and J. A. Spudich. 1990. The myosin stop size: measurements of the unit displacement per ATP hydrolyzed in an in vitro assay. *Proc. Natl. Acad. Sci. USA.* 87:7130–7134.

Toyoshima, Y. Y., S. J. Kron, E. M. McNally, K. R. Niebling, C. Toyoshima, and J. A. Spudich. 1987. Myosin subfragment-1 is sufficient to move actin filaments in vitro. *Nature.* 328:536–539.

Umemoto, S., and J. R. Sellers. 1990. Characterization of in vitro motility assays using smooth muscle and cytoplasmic myosins. *J. Biol. Chem.* 265:14864–14869.

Uyeda, T. Q. P., S. J. Kron, and J. A. Spudich. 1990. Myosin step size: estimation from slow sliding movement of actin over low densities of heavy meromyosin. *J. Mol. Biol.* 214:699–710.

Warrick, H. M., and J. A. Spudich. 1987. Myosin structure and function in cell motility. *Annu. Rev. Cell Biol.* 3:379–421.

Winkelmann, D. A., and S. Lowey. 1986. Probing myosin head structure with monoclonal antibodies. *J. Mol. Biol.* 188:595–612.

Winkelmann, D. A., S. Lowey, and J. L. Press. 1983. Monoclonal antibodies localize changes on myosin heavy chain isozymes during avian myogenesis. *Cell.* 34:295–306.

Winkelmann, D. A., F. Kinose, and A. L. Chung. 1993. Inhibition of actin filament movement by monoclonal antibodies against the motor domain of myosin. *J. Muscle Res. Cell Motil.* 14:452–467.

Winkelmann, D. A., L. Bourdieu, F. Kinose, and A. Libchaber. 1995. Motility assays using myosin attached to surfaces through specific binding to monoclonal antibodies. *Biophys. J.* 68:725.